

Efficient Data Generation for Stroke Classification via Multilayer Perceptron

*Original*

Efficient Data Generation for Stroke Classification via Multilayer Perceptron / Mariano, V., Tobon Vasquez, J.A., Casu, M.R., Vipiana, F.. - ELETTRONICO. - (2022), pp. 890-891. (2022 IEEE International Symposium on Antennas and Propagation and USNC-URSI Radio Science Meeting (AP-S/URSI) Denver, Colorado 10-15 July 2022) [10.1109/AP-S/USNC-URSI47032.2022.9886434].

*Availability:*

This version is available at: 11583/2971857 since: 2022-09-29T19:30:42Z

*Publisher:*

IEEE

*Published*

DOI:10.1109/AP-S/USNC-URSI47032.2022.9886434

*Terms of use:*

This article is made available under terms and conditions as specified in the corresponding bibliographic description in the repository

*Publisher copyright*

IEEE postprint/Author's Accepted Manuscript

©2022 IEEE. Personal use of this material is permitted. Permission from IEEE must be obtained for all other uses, in any current or future media, including reprinting/republishing this material for advertising or promotional purposes, creating new collecting works, for resale or lists, or reuse of any copyrighted component of this work in other works.

(Article begins on next page)

# Efficient Data Generation for Stroke Classification via Multilayer Perceptron

Valeria Mariano, Jorge A. Tobon Vasquez, Mario R. Casu, and Francesca Vipiana

Department of Electronics and Telecommunications, Politecnico di Torino, 10129 Torino, Italy, francesca.vipiana@polito.it

**Abstract**—The aim of this paper is to overcome one of the main problems of machine learning when it faces the medical world: the need of a large amount of data. Through the distorted Born approximation, the scattering parameters and the dielectric contrast in the domain of interest are linked by a linearized integral operator. This method allows to generate a large data-set in a short time. In this work, machine learning is exploited to classify brain stroke presence, typology and position. The classifier model is based on the multilayer perceptron algorithm and it is used firstly for validation and then with a testing set composed by full-wave simulations. In both cases, the model reaches very high level of accuracy.

## I. INTRODUCTION

Microwaves (MW) imaging and sensing techniques allow to obtain devices with a small size, low power intensity, portable and low cost. All these characteristics make this technology suitable for medical diagnostic of several diseases [1]. In particular, in this work, we are going to treat one of the main cause of human death: brain stroke.

In recent years, machine learning (ML) faces the medical world, and in this paper the background is the combination of MWI and ML, here some examples [2], [3]. However, the need of a huge amount of data for ML clashes with the difficulty in collecting a lot of medical data in a short time. Here, we try to overcome this incompatibility between these two worlds. In particular, we propose an alternative method to generate the data-set in a short time, through a linearized integral operator. Multilayer perceptron (MLP) is used for classification in validation and testing phase [4].

## II. MICROWAVE IMAGING SYSTEM

Fig. 1 depicts our Microwave Sensing system. We exploit a helmet composed of 24 flexible antennas, each acting as both transmitter and receiver. These antennas are placed in a thin dielectric layer that gives flexibility, increases the coupling, and facilitates field penetration through the head tissues. The position, the orientation, and the number of antennas are obtained with an optimization method that balances good performances and limited system complexity. Here, we use a working frequency equal to 1 GHz. In comparison with systems already in the literature [5], our approach reduces the overall size and increases matching and antennas attachment. The head in Fig. 1 represents the healthy condition and it contains a single material with head tissues average dielectric properties.

## III. DATA-SET GENERATION

In this section, there is the description of the process to generate the data-set, composed by 9 classes, which take into

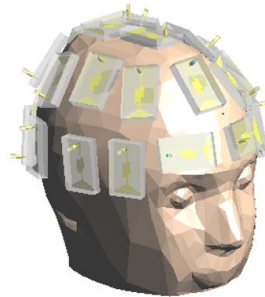


Fig. 1. MWI system CAD model.

account the presence, the typology and the position of the stroke. As shown in Fig. 2, the head is divided in 4 regions: front left (FL), front right (FR), back left (BL) and back right (BR). The data-set has 1 class for healthy case, and 4 classes for each type of stroke that identify the region.

The domain of interest (DoI), corresponding to the head, is discretized via tetrahedral cells. Each tetrahedron assumes the dielectric properties of the belonging tissue, depending on its position. The dielectric contrast is calculated considering the complex dielectric properties distribution of background ( $\epsilon_b(\underline{r})$ ) and the case of interest ( $\epsilon_r(\underline{r})$ ):

$$\Delta\chi(\underline{r}) \triangleq \frac{\epsilon_r(\underline{r}) - \epsilon_b(\underline{r})}{\epsilon_b(\underline{r})}, \quad (1)$$

For each pair of antennas  $j$  and  $k$ , this is the linearized integral equation that links the dielectric contrast  $\Delta\chi$  with the differential scattering parameters  $\Delta S$ , exploiting the distorted Born approximation:

$$\Delta S_{j,k} = -\frac{j\omega\epsilon_b(\underline{r})}{2a_j a_k} \iiint_V \underline{E}_{b,j}(\underline{r}) \cdot \underline{E}_{b,k}(\underline{r}) \Delta\chi(\underline{r}) d\underline{r} \quad (2)$$

where,  $\underline{E}_b(\underline{r})$  is the field radiated in  $\underline{r}$ ,  $a$  is the power waves at antennas port,  $\omega$  is the angular frequency and  $V$  is the DoI volume. Finally,  $\Delta S$  is the difference between the scattering parameters at antennas ports with and without the stroke.

The first step is the positioning of a spherical stroke in the head, randomly choosing the center among the tetrahedra barycenters and changing the dielectric properties of the tetrahedra with a distance from the center smaller than the considered radius. The stroke can have 5 different dimensions, coherent with realistic cases: radius equal to 1, 1.5, 2, 2.5, 3 cm. Once the tetrahedra belonging to the stroke have been defined, we can calculate the dielectric contrast through (1).

The second step, after the positioning of the stroke, is the addition of white noise to the dielectric contrast with 4 different levels that cause the following noise thresholds on  $\Delta S$ : -110, -105, -95, -90 dB.

Now, for each pair of antennas, we calculate  $\Delta S$  through (2). The features of the data-set are the scattering parameters obtained adding  $S^{inc}$  (scenario without the stroke) to  $\Delta S$ . Since, the S matrix is symmetrical, we select only the upper triangular matrix. Moreover, the real and the imaginary part of S parameters are considered as 2 different features, for a total of 600 features. The data-set comprises 10000 samples, almost equally distributed among the classes. Through this method, the S parameters are comparable to the ones obtained with full-wave simulations, but with a reduction of generation time equal to 3 orders of magnitude.

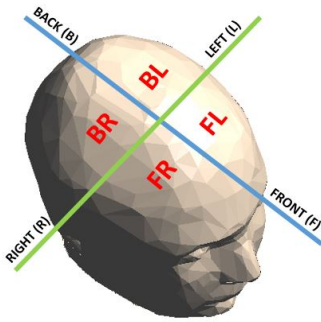


Fig. 2. Head subdivision: front left (FL), front right (FR), back left (BL) and back right (BR).

#### IV. NUMERICAL RESULTS

In this section there are the results obtained with MLP algorithm. The first test is validation in which the data-set is divided into training set (80% data-set) and validation set (20% data-set). The hyperparameters of MLP are selected through the grid search technique [6]. The neural network is composed by 5 hidden layers (1000, 500, 250, 100 and 50 neurons). It exploits as activation function the hyperbolic tangent, the solver stochastic gradient descent and the regularization term  $\alpha = 0.0001$  [4]. After the training, the model classifies the validation set with an accuracy equal to 97.90%.

The next step is the analysis of the algorithm model performances with a testing set composed by full-wave simulations, obtained through a finite element method (FEM) solver [7]. In this phase, the stroke can assume 2 different shapes (sphere and ellipsoid) with different dimensions comparable with the ones exploited in the training set. In the testing set for each class, there are a few samples. For each of them we obtain further samples by adding 4 different levels of noise obtained mapping the noise on dielectric contrast space ( $\delta\chi$ ) to the differential scattering parameters space ( $\delta S$ ), with (2). Through this method we generate a testing set with a total of 140 samples.

In Fig. 3, the confusion matrix with on the rows the true labels and on the column the predicted labels. The squares

identify the 3 macro-classes: yellow for healthy case, green for ischemic stroke and red for hemorrhagic stroke. The results in Fig. 3 shows that the algorithm always correctly classifies the macro-class, but in some critical cases it assigns to the stroke a wrong position, in that cases the center of the stroke is really close to one of the head axis.

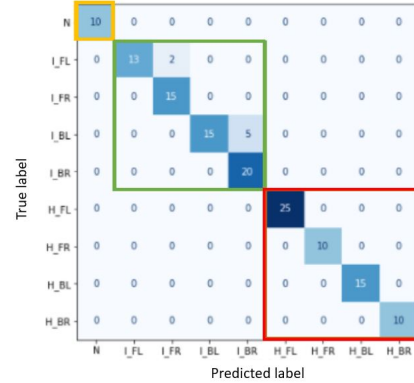


Fig. 3. Confusion matrix with testing phase results. The 3 squares identify the macroclasses: yellow for healthy case, green for ischemic and red for hemorrhagic stroke

#### V. CONCLUSION AND PERSPECTIVES

In this paper, we have proposed an efficient method to generate a large amount of different simulated data in a short time. Applying the Born approximation, the dielectric contrast in the DoI is linked with the differential scattering parameters through a linearized integral operator. The ML model is based on MLP algorithm and it reaches good performances in both validation and testing phase. The future step will be the use of the same algorithm model to classify measurements data.

#### ACKNOWLEDGEMENT

This work was supported by the MIUR under the PRIN project “MiBraScan”, and by the European Union’s Horizon 2020 Research and Innovation Program under the EMERALD project, grant agreement No. 764479.

#### REFERENCES

- [1] L. Crocco, I. Karanasiou, M. James, and R. C. Conceicao (Eds.), *Emerging Electromagnetic Technologies for Brain Diseases Diagnostics, Monitoring and Therapy*. Springer int. pub., 2018.
- [2] G. Zhu, A. Bialkowski, L. Guo, B. Mohammed, and A. Abbosh, “Stroke classification in simulated electromagnetic imaging using graph approaches,” *IEEE J. Electromagn., RF, Microw. Med. Biol.*, vol. 5, no. 1, pp. 46–53, 2021.
- [3] M. Salucci, A. Polo, and J. Vrba, “Multi-step learning-by-examples strategy for real-time brain stroke microwave scattering data inversion,” *Electronics*, vol. 10, no. 1, 2021.
- [4] M. A. Nielsen, *Neural Networks and Deep Learning*. 2019.
- [5] J. A. Tobon Vasquez *et al.*, “A prototype microwave system for 3D brain stroke imaging,” *Sensors*, vol. 20, May 2020.
- [6] Y. LeCun, L. Bottou, G. Orr, and K. Muller, “Efficient backprop,” in *Neural Networks: Tricks of the Trade* (G. Montavon, G. B. Orr, and K.-R. Müller, eds.), ch. 1, pp. 9–48, Springer int. pub., 1998.
- [7] D. O. Rodriguez-Duarte, J. A. Tobon Vasquez, R. Scapaticci, L. Crocco, and F. Vipiana, “Assessing a microwave imaging system for brain stroke monitoring via high fidelity numerical modelling,” *IEEE J. Electromagn., RF, Microw. Med. Biol.*, pp. 1–1, 2021.